Article (refereed) - postprint

Dry corridors opened by fire and low CO_2 in Amazonian rainforest during the Last Glacial Maximum

Hiromitsu Sato[1], Douglas I. Kelley[2], Stephen J. Mayor[3],
Maria Martin Calvo[4], Sharon A. Cowling[5], Iain Colin Prentice[6] *

April 3, 2021

1 Abstract

The dynamics of Amazonian rainforest over long timescales connects closely to its rich biodiversity. While palaeoecological studies have suggested its stability through the Pleistocene, palaeontological evidence indicates the past existence of major expansions of savanna and grassland. Here we present integrated modeling evidence for a grassier Neotropics during the Last Glacial Maximum (LGM), congruent with palaeoecological and biological studies. Vegetation reconstructions were generated using the Land Processes and eXchanges (LPX) model, driven by model reconstructions of LGM climate, and compared against palynological data. A factorial experiment was performed to quantify the impacts of fire and low CO_2 on vegetation and model-data agreement. Fire and low CO_2 both individually and interactively induced widespread expansion of savanna and grassland biomes while improving model-data agreement. The interactive effects of fire and low CO_2 induced the greatest 'savannafication' of the Neotropics, providing integrated evidence for a number of biogeographically relevant open vegetation formations including two dry corridors; paths of savanna and grassland through and around Amazonia that facilitated major dispersal

*Affiliations: 1. University of Toronto 2. Centre of Ecology and Hydrology, Wallingford 3. Ontario Forest Research Institute, Ontario Ministry of Natural Resources and Forestry 4. Imperial College London 5. University of Toronto 6. Imperial College London

and evolutionary diversification events. Our results show a bimodality in tree cover that was driven by fire and further enhanced by 'CO$_2$ deprivation', which suggests biome instability in this region of climate space.

Main Text

Biotic diversification in the Neotropics has been hypothesized to rely on broad changes in vegetation, which induce large-scale processes such as dispersal, vicariance, and speciation [35]. The Refugia Hypothesis postulates that Amazonian rainforest was fragmented into disjunct 'refugia' by tracts of savanna during Pleistocene glacial periods. This fragmentation would be sufficient to inhibit gene flow between refugia, allowing speciation. Forests would expand and reconnect during interglacials, leading to range expansion of the newly diversified taxa [20]. Diversification in the Atlantic forest region in southeastern Brazil has also been attributed to refugia dynamics [9].

A number of palaeoecological studies have contradicted the Refugia Hypothesis [11][4][5], claiming that Amazonian forests remained intact over Pleistocene climatic fluctuations. These studies are broadly consistent with some past model reconstructions [14][10][36][23], which show Amazonian forest during the LGM to be similar in extent relative to its pre-Industrial status. However, these studies relied on climatic factors only in their reconstructions, performed without explicit examination of the effects of non-climatic factors such as fire and CO$_2$. Furthermore, recent palynological studies have found savanna-like vegetation during the late Pleistocene within current Amazonian forest [22][18]. Re-evaluation of the Lake Pata records has also challenged the notion of stable moist forest even within the basin over glaciations, finding discontinuities and significant compositional changes during the last glacial period [17]. The degree of 'savannafication' of the glacial Neotropics is thus largely unknown due to the scarcity of pollen cores that date back to the LGM.

Disjunct distributions of species associated with semi-arid biomes also sug-

gest the past presence of open vegetation biomes in regions that are currently occupied by closed canopy tropical forest [41][38]. Three past savanna formations, referred to as 'dry corridors', have been hypothesized to explain past connectivity between the northern and southern savanna regions of South America [8][16][41][48]. The central Amazonian corridor would extend diagonally northwest to southeast from the savannas in the northern Amazonian border to those central Brazil, along an extensive tract of forest that currently experiences a significant degree of seasonality in precipitation [50]. The circum-Amazonian corridor, also known as the Andean corridor, would have existed along the Andes and western border of Amazonian forests, while the coastal corridor has been hypothesized to have existed along the Atlantic coast.

Here, we estimated the effects of fire processes and CO_2 on vegetation in the Neotropics during the LGM, addressing the stability of biomes under glacial conditions using a comprehensive process-based model. Emphasis was placed on estimating the isolated and interactive effects of fire and low CO_2 on biome distribution and tree cover. A factorial experiment was conducted to elucidate these effects, consisting of four scenarios all driven by LGM climate: pre-Industrial CO_2 (280 ppm) without fire processes (*control*), pre-Industrial CO_2 (280 ppm) with fire processes (*fire only*), LGM CO_2 (180 ppm) without fire processes (*low CO_2 only*), and LGM CO_2 (180 ppm) with fire processes (*fire and low CO_2*).

To account for variability among climate models, four distinct model reconstructions of LGM climate were used to drive the Land surface Processes and eXchanges (LPX) [40]. The outputs from all four of the LGM climate reconstructions were then averaged to create an ensemble data set that was also subject to analysis. Each scenario from the five sets of vegetation reconstructions was then compared against palynological data to assess model-data agreement.

Comparing Model Reconstructions to Palynological Data

The activation of fire and low CO_2 resulted in small but consistent improvements in agreement between model reconstructions of LGM vegetation and palynological data (42 cores). Expansion of open biomes and displacement of forest underlie these improvements. Model-data agreement was further improved by the simultaneous activation of fire and CO_2 relative to control for all five experiments, four of which were deemed statistically distinct from the ensemble experiment according to a paired student t-test (fig. 2). Pollen-derived biomes were compared against model reconstructed biomes quantitatively using the Discrete Manhattan Metric (DMM) by assessing the net distance between biomes' ecological affinities at each site (methods). The activation of fire (*fire only*) and the imposition of low CO_2 (*low CO_2 only*) in isolation both improved model-data agreement, though fire activation consistently improved DMM scores more than low CO_2. The simultaneous inclusion of fire processes and low CO_2 (*fire and low CO_2*) resulted in the lowest average DMM and highest model-data agreement, highlighting the importance of their combined effects.

Variations between LGM climate reconstructions were reflected in model-data agreement, though almost all AOGCM runs showed similar relative performance within their factorial experiments (fig. 2). The control scenario had lowest data-model agreement, followed by *fire only* and *low CO_2 only* scenarios, with *fire and low CO_2* having the highest relative model-data agreement save for FGOALS-1.0g. Of the twenty model vegetation reconstructions, the ensemble *fire-and-low CO_2* run agreed most with palynological data. The degree of testing rigor is limited by the number and locations of suitable pollen cores, which are rare in Amazonia due to poor preservation conditions. Though the distribution of cores is thus far insufficient for a basin-wide test, such comparisons can effectively identify physical processes and model skill at the local and regional scale.

4

Fire and Low CO_2 Drove Expansions of Grasslands

Fire and low CO_2 had considerable effects on model reconstructions of vegetation, potentially outweighing the effects of glacial climate as examined by previous studies [36][23]. Relative to control, wildfire at pre-Industral CO_2 (*fire only* scenario) showed a general shift to biomes associated with increased aridity. Tropical moist forest was reduced by 11% relative to control (7.6 million km^2 vs 8.6 million km^2), which was replaced predominantly by savanna (fig. 1 a, b). Warm temperate forest, most of which was Atlantic forest, also showed reductions in area and were replaced by sclerophyll woodland. Area occupied by grassland in the *fire only* scenario (4.2 million km^2) was 350% greater than that of control (1.2 million km^2), replacing savanna in the current caatinga of Northeastern Brazil and woodland and parkland in and adjacent to the Pampas region in the south. In northern Colombia and Venezuela, fire was found to induce desert where savanna and grassland occupied in the control.

The effects of low CO_2 (*low CO_2 only* scenario) appear to have a generally similar effect on biome distributions as fire: forest biomes are reduced in extent by intrusions of open vegetation biomes (fig. 1 a, c). Low CO_2 induced shifts in biomes similar to that of the *fire only* scenario. However, unlike fire, low CO_2 replaced entire regions of tropical dry forest with savanna and grassland. Tropical moist forest was reduced by 13% relative to control, from 8.5 million km^2 to 7.4 million km^2. Low CO_2 also induced significant expansion of grassland regions.

The combined effect of fire and low CO_2 had the strongest impacts on biome distribution relative to control. Reductions in forest area were dramatic as were expansions of open vegetation biomes, including regions that were unaffected by either factor in isolation. Amazonian forest contracted significantly, particularly the southern margins. Savanna and grassland showed extensive intrusion into the central Amazonian corridor region, with small patches of isolated savanna of various size within the forest. Tropical forest in the *fire and low CO_2* scenario occupied 56% of the area (4.8 million km^2) relative to control (8.5 million km^2).

5

Warm temperate forest, which represents Atlantic forests, occupied only 15% of the area relative to control. Conversely, grassland expanded by 550% relative to control (6.6 million km^2 vs. 1.2 million km^2), occurring in large patches in the mosaic of open canopy biomes that comprise the majority of the *fire and low CO_2* scenario.

These trends were consistent among all LGM model reconstructions driven by the four climate reconstructions, though with significant variation. Amazonian rainforests remained vast and continuous in scenarios in *fire only* and *low CO_2 only* scenarios, consistent with past modeling studies [14][10][36][23]. It is only with both effects simultaneously activated that our reconstructions diverge from past modeling studies.

Whittaker plots for model runs were generated to examine the effects of low CO_2 and fire on climate-vegetation relations (fig. 4), showing the location of biomes in climate space. Scenarios without fire tend to have biomes that occupy clearly defined areas of climatic space. The presence of fire tends to obscure these well-defined boundaries. The expansion of grassland is a clear effect of fire, which is well-reflected in its broad and speckled climate-space distribution. Low CO_2 tends to reduce the area of climate-space of all major forest types, allowing savanna to encroach into the climate-space of tropical moist and dry forest and sclerophyll woodland to encroach into that of warm temperate forest. The combined effect of low CO_2 and fire compounds these two effects, resulting in much reduced climate-space of forest biomes while expanding that of grassland (fig. 4 a,d).

Interactive Effects of Fire and Low CO_2

To discern the individual and interactive effects of fire and CO_2 on tree cover, a Stein-Alpert factor separation was performed on the ensemble experiment (methods). Individually, fire and low CO_2 had showed similar effects on tree cover, inducing large reductions in most of Central and South America, while having little to no effect on Amazonia (fig. 5 a,b). Low CO_2 individually had

6

broader effects on tree cover, showing small reductions in the central dry corridor regions of Amazonia and major reductions in southeast of Brazil (fig. 5 a, c). Interactions between fire and low CO_2 resulted in enhanced tree cover loss in several regions, including the northern savanna of Colombia and Venezuela and large patches of Amazonia in central Brazil (fig. 5 a, d).

In the control scenario, a spectrum of tree cover occurred over regions of intermediate precipitation (0 - 2000 mm) (fig. 6 a). Intermediate tree cover (30 - 60 %) is present, showing little if any sign of bimodality of tree cover. The activation of low CO_2 tends to reduce the density of very high tree cover ($\sim$ 0.95), likely expressing reductions of tree cover even in regions that receive ample precipitation (fig. 6 c). The activation of fire results in low tree cover even in regions of high precipitation, relative to control (fig. 5 b). Fire also has another distinct effect on tree cover: intermediate tree cover is less frequent and the spectrum of tree cover is shaped into a stronger bimodality. The fire-forced bimodality of tree cover is further enhanced by the simultaneous activation of low CO_2 and fire, showing more distinct reductions of intermediate tree cover over a broader range of precipitation (fig. 6 d).

Open Dry Corridors and Forest Stability

A number of hypothesized formations of open vegetation, including two dry corridors, were identified in our model reconstructions (fig. 3). Indications of a central Amazonian corridor appeared in a number of model runs, showing almost full connectivity in the ensemble *fire and low CO_2* scenario, which had the highest agreement with pollen records. In this run, savanna significantly expanded through the southeast margins of Amazonia to connect with the non-forested biomes in the far north. A narrow, continuous tract of savanna and grassland resembling a circum-Amazonian dry corridor was also reconstructed in a number of runs, also most prominent in *fire and low CO_2* scenarios. Moist forest remained robust along the Atlantic coast in northern Brazil, showing no indication of a trans-Amazonian Atlantic corridor at the biome level. However,

7

canopy density and height were slightly reduced according to the ensemble vegetation reconstruction (fig. ED1, ED2), suggesting a degree of openness in the region. It is notable that the broad savannafication required to open the central Amazonian dry corridor seems contingent on the interactive effects of fire and low CO_2, while both the individual and interactive effects of fire and low CO_2 induce opening of the circum-Amazonian corridor.

Atlantic forests were found to be present but heavily reduced in size and restricted to the Brazilian coast, consistent with phylogeographic and statistical modeling work of Carnaval and Moritz [9]. The Pernambuco and Bahia refuges were both present in the *fire and low CO_2* reconstruction, separated from one another by tropical savanna.

The effects of wildfire and low CO_2 consistently improved model-data agreement, suggesting their potential importance in determining vegetation in the LGM Neotropics. Both fire and low CO_2 induced expansions of open vegetation biomes such as savanna and grassland while reducing forested area, particularly in Amazonia. Though reduced in size, Amazonian rain forest remained largely continuous with a stable western core. Thus, we conclude that vegetation in LGM Neotropics may have been more open than previously thought, with significantly less forest and significantly more mosaics of grassy biomes. A number of areas, including large regions in the southern margins of Amazonia and central corridor location, show marked instability with regard to changes in climate, low CO_2, and fire regime.

Past refutations of widespread glacial savannafication were often based on single or a small number of study sites [12][6], and were likely insufficient to conclusively exclude savanna and grassland expansion at the regional-scale. Moist tropical forest was correctly reconstructed at the Lake Pata site in all twenty LGM vegetation reconstructions performed in our study, though with significant variation in extent and shape of Amazonian rainforest. Existing refutations have not addressed more recent pollen studies in the approximate central corridor and Amazonian southern margin, such as the Serra Sul Carajas and Lago

do Saci cores, that are interrupted by sedimentary hiatuses around the LGM or suggest savanna during the LGM [22][18]. Past regional modeling studies that suggested that Amazonia was robust during the LGM were performed using equilibrium models, which lacked fire representation and its interactions with low CO_2 [14][30]. Statistical reconstructions of biome distributions during the LGM are based on the assumption that climate solely controls vegetation distribution, and also neglect the effects of low CO_2 and fire [48][13].

Interactive Stressors on Neotropical Trees

Our results are also consistent with two prominent ecological theories: the fire-driven bimodality of tree cover and the expansion of grasses due to low CO_2. Our results also emphasize the oft-neglected but potentially critical role of non-climatic drivers on vegetation cover in palaeoecological contexts. Within the context of the LGM, low CO_2 gave grasses a competitive advantage over trees, compounded by the effects of fire, and worsened by aridity. These processes would better explain palaeoecological evidence of a largely grassier South America during the LGM, which was overall more vulnerable to intrusions by savanna. Fire was found to be a driving factor in the bimodality of tree cover, with enhanced efficacy at lower levels of CO_2; a potentially significant interaction between fire and 'CO_2 deprivation'. While bimodality of tree cover exists in regions of intermediate precipitation, this is not proof that forest and savanna are alternate stable states, as MAP is too coarse a measure of environmental niche. However, this bimodality of tree cover does indicate instability in this region of climate space, where small changes in growing conditions may lead to large changes in tree cover. In this case, fire may induce a positive feedback in reducing tree cover, where the initial fire-driven proliferation of grasses leads to faster accumulation of dry fuel to drive further fires [49]. Similar results have been derived from simulations of climate change in Africa, where CO_2 and its interactions with fire were found to have major impact on determination of savanna and forest biomes [33]

9

There are a number of broad implications if fire and CO_2 are indeed important determinants of terrestrial vegetation. Even when driven by identical climate scenarios, modifications of CO_2 and fire regime can significantly alter structure and distributions of terrestrial vegetation. Relations between vegetation and climate are sensitive to non-climatic factors and dynamic through time due to fluctuating CO_2. Burbridge et al. suggested the likely role of low CO2 in LGM expansion of dry forest and savanna in Bolivian Amazonia, which is consistent with our findings [4]. We thus recommended greater consideration of non-climatic processes such as fire and CO2 in palynological reconstructions, particularly in ecotonal regions. Similarly, ecological niche modeling studies which also assume robust, stable relationships between vegetation and climate, may also face this issue if reconstructing vegetation over geologic time. Without accounting for fire and low CO_2 in glacial periods, stability of forest biomes may be overestimated and vegetation-mediated diversification processes may be obscured.

Biogeographical Implications

A major consequence of our study was the modeled reconstructions of a number of biologically-significant formations including the central Amazonian and circum-Amazonian dry corridors and Atlantic forest refugia. There is currently no suitable palynological data from the core of the central northwest-southeast savanna corridor, which limits our ability to conclusively determine its past existence and motivates contextualization of our results with biogeographical studies. Our model reconstructions of a central Amazonian dry corridor are congruent with molecular genetic studies of the Neotropical rattlesnake (Crotalus durissus), which occupies seasonal habitats ranging from Mexico to Argentina [41]. Though widespread through the Neotropics, they are absent in Amazonian and Central American moist forest and have generally disjunct distributions. Phylogeographic analysis suggests a progressive, step-wise colonization from Central America to the southeast Brazil traversing the Amazon basin. While

divergences in Central American clades were likely to have occurred in the late Miocene or early Pliocene, trans-Amazonian vicariant cladogenesis likely occurred more recently in the mid-Pleistocene [50]. This in turn would require a 'shrunk or fragmented' Amazonian forest that gives way to seasonal or open vegetation formations that could act as continuous corridors for dispersal.

Though the value of establishing the evolutionary history of Neotropical biota within the context of Earth history has been recognized [1][37], actual research aimed at integration has been curbed by the spatial and temporal limitations of palaeoecological data [27]. Process-based modeling, particularly when grounded in empirical data, offers extensive and continuous reconstructions of past environments that can justifiably interpolate between data sites.

A mechanistic understanding of glacial period savannafications could have important consequences, with conceptual similarities to Haffer's model of Pleistocene diversification [21][19]. During glacial periods, open vegetation corridors would emerge and induce dispersal and range expansion for savanna and grassland adapted taxa. During interglacials, forest would replace open biomes and dry corridors would close, inducing vicariance (geographical separation of populations) and differentiation. Conversely, a broad central Amazonian non-forested corridor could feasibly act as a barrier and isolate populations of moist forest taxa at opposing sides of the corridor inducing diversification. Closing of corridors during interglacials would then allow the newly diversified moist forest taxa to disperse and expand their ranges. This process could be cyclic, following Pleistocene climatic fluctuations, and act as a two-way pump or 'accordion'. This would allow periodic and rapid diversification, given that each phase leads to vicariance of taxa of alternating forest and savanna niches. This is consistent with existing theories of alternating moist and dry habitat corridor and evidence of sustained diversfication of both moist forest and arid-adapted species during the Pleistocene [45]. It is noteworthy that gallery rainforests along the Amazon river could persist during dry periods and act as a migration corridor for moist forest species, which could compromise the effectiveness of a central

11

dry corridor. While the duration and extent of corridor may not permit full speciation, this process could drive recent intraspecific genetic diversification. This unique confluence of factors involving the geography of the Neotropics and Pleistocene climatic oscillations may have contributed to an accumulation of biological diversity.

Methods

Model Description and Protocol

Dynamic Global Vegetation Models (DGVMs) simulate spatially and temporally resolved potential vegetation and ecosystem structure (e.g. height, biomass, leaf area index and foliage projective cover) and function (e.g. biogeochemical carbon and water fluxes and disturbance) via a number of competing Plant Functional Types (PFTs). These models, therefore, provide an integrated, process-based way to estimate the impacts of climate changes on terrestrial ecosystems [15][44]. This includes hindcasts of past impacts of climatic change on the Earth's land surface to complement palaeoecological data, which also serves to ground-truth models over long timescales [32].

The DGVM used for this study, Land surfaces Processes and eXchanges (LPX) [40], is a descendant of the widely used Lund-Potsdam-Jena DGVM [43] coupled to the processed based SPread and InTensity of FIRE model (LPJ-SPITFIRE) [47]. PFTs in LPX are initially defined by life form (i.e woody plant or grass). Trees PFTs are then split by climate range (tropical, temperate, boreal) leaf type (broad or needle leaf), and phenological response (evergreen, raingreen or summergreen). Grasses are split by C3 and C4 photosynthetic pathways. LPX uses a photosynthesis-water balance scheme that couples CO_2 assimilation with transpiration. Reduced CO_2 concentrations, such as those during the LGM, increases potential water stress on plants by increasing the required stomatal conductance (g_c) for the same photosynthetic rate. The maximum, unlimited potential stomatal conductance ($g_{c,max}$) is determined by the

12

maximum potential day-time photosynthetic assimilation rate (A_{max}), ambient CO_2 concentration, PFT-specific minimum canopy conductance and, for grasses, photosynthetic pathway. If $g_{c,max}$ results in a maximum transpiration demand (D) that is greater than the supply of water from the soil (S - calculated from soil water content and soil properties), then g_c - and therefore photosynthesis - is reduced so that transpiration is equal to S, as described by Monteith [34]. When CO_2 is decreased, $g_{c,max}$ increases even if A_{max} is unchanged, and the value of S that induces water stress is increased - i.e maximum photosynthesis only occurs at higher soil moisture. Photosynthesis is also reduced by a greater amount than with higher CO2 if S is less than D.

In LPX's process-based fire model [40], fire occurrence is a product of ignitions represented by lightning, the mean probability of ignition calculated from local fuel and atmospheric moisture content, and fire susceptibility based on fuel amount, fuel properties and fuel moisture content. Fires that do start have a rate of spread, flame height and residence time are based on weather conditions and fuel moisture, and calculated using the Rothermel equations [42]. Burnt area is the product of the number of fires and the average spread of fire. PFT mortality in a given area burnt can occur from either cambial damage and/or crown scorching. Cambial damage increases with fire intensity and residence time, but is resisted by the PFTs local bark thickness, and thicker-barked trees surviving longer, more intense fires. Bark thickness is related to PFT height via a PFT-specific allometry relationship. The impact of crown scorching is determined by fire intensity and height in relation to the height of the locally simulated PFTs. Crown scorch mortality increases as flame height increased above canopy height of each PFT. LPX its simulated fire regimes have been extensively ground-truthed against modern data [39][40][24][25][26], which made it a particularly suitable model for the purposes of this study. A more comprehensive descriptions of LPX and its components can be found in [40][24][47].

13

LGM Climate Scenarios and Modeling Protocol

Inputs reflecting the LGM climate were derived from four atmosphere-ocean general circulation model (AOGCM) datasets (MIROC3.2, FGOALS-1.0g, HadCM3M2, CNRM-CM33) produced by the Palaeoclimate Modelling Intercomparison Project Phase II (PMIP2) [2]. Boundary conditions (ice sheets, coastlines, greenhouse gas concentrations, eccentricity, obliquity, and angular precession) for these runs are described in [2]. These datasets were also used to drive previous global-scale reconstructions of LGM vegetation [39][7]. Atmospheric CO_2 was set to 185 ppm in accordance with the PMIP2 protocol for all runs [3].

Several steps were required to prepare these model scenarios for compatibility with LPX. Differences between LGM climate scenarios and a Pre-Industrial Holocene baseline climate variables ('anomalies'), were superimposed onto a $0.5° \times 0.5°$ grid Pre-Industrial climate scenario (Climate Research Unit Version 3.0, detrended data from 1900-1950). Climate data with superimposed anomalies was then extrapolated onto the exposed continental shelf and removed from regions covered by ice sheets characterisitic of the LGM.

For all model simulations, 'spin-ups' from bare ground were ran for 4000 years and main runs for 1380 years. Equilibrium tests were performed on each data set to check for the temporal stability of output variables (fig. S3). If for the majority of grid cells, canopy density (Leaf Area Index - LAI) and foliage projective cover (fpc) showed less than 2% variation relative to the previous time step, equilibrium was taken to have been reached. Model output for the last 138 years (length of base Pre-Industrial data set) was averaged and used for reconstructions of LGM vegetation.

LPX Biome Assignment

Biome assignment was implemented through post-processing of three LPX outputs: Growing Degree Days (GDD), vegetation height, and foliage projective cover (fpc) (fig. S4). The biome assignment scheme used in this study is identical to that of Prentice et al. [39] and Calvo et al. [7], save a refinement to

14

distinguish seasonal and evergreen forests. A threshold of mean annual GDD (above 5°C) was set to 350°C·days to separate cold biomes from their warm and tropical counterparts (ex. tundra vs desert). Height and fpc are then used to distinguish between bareground, grassland, savanna, and forest biomes. The presence or dominance of PFTs within a grid cell then determines its assignment as tropical, boreal or temperate. Forests are classified as either seasonal or evergreen based on the relative proportions of summergreen, raingreen, and evergreen forest pfts.

Model-Pollen Biome Correspondence

The definitions of South American biomes, their correspondence to pollen spectra, and LGM biome reconstructions were based on a comprehensive meta-analyses by Mayle et al. [23] and Marchant et. al [28] in addition to the original studies (Extended Data - table 1). Pollen-based biomes and the model-outputs rarely have a simple one-to-one correspondence, given that vegetation model biomes are often developed for global application, while pollen-based biome reconstructions are refined to more subtle regional or local definitions. Model-data comparison was perfomed using the Discrete Manhattan Metric (DMM) applied to the four fire/CO_2 scenarios for five climate reconstruction inputs (four AOGCM climate reconstructions and one ensemble) for a total of twenty cases. The DMM characterizes biomes through bioclimatic and ecophysiological traits, permitting a quantification scheme to rate the 'distance' between two biomes. The scores for each scenario represents the average distance, with smaller values indicating higher average agreement between model and pollen reconstructions.

Discrete Manhattan Metric

Discrete Manhattan Metric

The 'Discrete Manhattan Metric' (DMM) was developed to quantify the distance or 'closeness' between biomes, permitting direct comparison between model out-

put and pollen records and a measure of overall model-data agreement. Each biome has a set of ecophysiological affinities, represented by a discrete number, resulting in an *affinity matrix* (fig. 4). Given two biomes, each having an affinity for each trait represented by a number between zero and one, we find their 'ecological distance' by: 1) calculating the difference in their affinity scores for each trait 2) summing the magnitude of these differences 3) normalizing by the total number of traits.

The x_{ij} element of affinity matrix, X_{MN} (Extended Data - table 2), is the affinity for the ith biome to the jth trait for N biomes and M traits. The distance, $d(a,b)$ between two biomes (indexed by a and b) is the sum of the differences in traits, normalized by the total number of traits N (eq. 1).

$$d(a,b) = \sum_{j=1}^{N} |x_{aj} - x_{bj}|/N \qquad (1)$$

In the case where the biomes are the same, their distance between then is equal to 0. If the biomes are maximally different (ex. tropical rainforest and tundra), their distance is equal to 1. This process would be repeated for every pollen-core site, where the modeled biome reconstruction for that point would be tested against the pollen-based reconstruction. Model performance is thus the mean of the scores for each pollen site, multiplied by two to remain consistent with properties of the continuous Manhattan Metric used in modern benchmarking [24]. A paired student t-test was performed on all 20 model-data comparisons to determine the likelihood of equality between mean scores with a p-value cutoff of 0.05.

The correspondence between the LPX biome assignment scheme and pollen-based biomes were based on meta-analysis by Mayle et al. [23], Marchant et al. [28], and the original palaeoecological studies. A number of major pollen-reconstructed biome under examination had natural correspondences with model assigned biomes, while others were more subtle and open to interpretation (Extended Data - table 3). For example, tropical rainforest and dry forest from

pollen studies had a natural correspondence to tropical humid forest and tropical dry forest in LPX, while the various reconstructions of open, non-analogue vegetation sites were more difficult to categorize in terms of model biomes. While correspondences may be rudimentary, the impact of errors in categorization would be softened by the design of the DMM, as opposed to a direct binary metric. Moreover, our study developed and applied a scheme to quantify model-data agreement between DGVM output and pollen data, which is rarely attempted despite its importance. Further details and references to original studies for each core site are located in the 'core list' (Extended Data - table 1).

Stein-Alpert Decomposition

A Stein-Alpert decomposition was designed to compute isolated and synergistic effects of factors within numerical simulations [46] . Though initially developed for atmospheric models, this factor separation scheme can be adapted for climatic and non-climatic factors within vegetation models. In our decomposition, f_0, f_1, f_2, and f_{12} are fields composed of tree cover outputs from the ensemble climate reconstruction for the *control*, *low CO_2 only*, *fire only*, and *fire and low CO_2* (eq. 2-5) scenarios respectively.

$$f_0 : \text{fire off, Pre-Industrial CO}_2 \tag{2}$$

$$f_1 : \text{fire off, \textbf{LGM CO}}_2 \tag{3}$$

$$f_2 : \textbf{fire on}, \text{PI CO}_2 \tag{4}$$

$$f_{12} : \textbf{fire on, LGM CO}_2 \tag{5}$$

Effects from the factors of fire and CO_2 are calculated by addition and subtraction of the fields. The isolated effect of fire is the difference between the tree

17

cover from the *fire only* and the *control* scenarios (eq. 6). Similarly, the isolated effect of low CO_2 is the difference between the *low CO_2 only* and *control* scenario (eq. 7). The simultaneous effect of both fire and low CO_2 is represented by $< f_3 >$, which is not a component of a formal Stein-Alpert decomposition (eq. 8). The synergistic effects of fire and CO_2 are computed by subtracting both the tree cover from the *fire only* and *low CO_2 only* scenarios from the *fire and low CO_2* scenario while adding the tree cover from the *control* scenario (eq. 9).

$$< f_1 >= f_1 - f_0 \tag{6}$$

$$< f_2 >= f_2 - f_0 \tag{7}$$

$$< f_3 >= f_{12} - f_0 \tag{8}$$

$$< f_{12} >= f_{12} - (f_1 + f_2) + f_0 \tag{9}$$

A logit transformation was performed on the tree cover fields f_i to convert the bounded variable of tree cover (ranging from 0 to 1) to an unbounded variables (ranging from $-\infty$ to ∞) (refer to eq. 10 - 12). For a bounded variable y, which in our case are values of tree cover within each grid cells of a scenario, equation 10 to 11 are applied to create an unbounded transformed variable y_2, which undergoes the arithmetic of the Stein Alpert decomposition. Equation 10 was used to transform the bounds of tree cover from [0,1] to (0,1), as is required for the logit transformation of equation 11. Afterward the arithmetic is performed, equation 12 is used to transform y_2 back to the initial bounded variable y.

$$y_1 = (99y + 0.5)/100 \tag{10}$$

18

$$y_2 = log(y_1/(1 - y_1)) \tag{11}$$

$$y = 2/(1 + e^{-y_2}) - 1.0 \tag{12}$$

References

[1] Aleixo, A., & de Fátima Rossetti, D. (2007). Avian gene trees, landscape evolution, and geology: towards a modern synthesis of Amazonian historical biogeography?. Journal of Ornithology, 148(2), 443-453.

[2] Braconnot, P., Otto-Bliesner, B., Harrison, S., Joussaume, S., Peterchmitt, J. Y., Abe-Ouchi, A., ... & Kageyama, M. (2007). Results of PMIP2 coupled simulations of the Mid-Holocene and Last Glacial Maximum–Part 1: experiments and large-scale features. Climate of the Past, 3(2), 261-277.

[3] Braconnot, P., Otto-Bliesner, B., Harrison, S., Joussaume, S., Peterchmitt, J. Y., Abe-Ouchi, A., ... & Kageyama, M. (2007). Results of PMIP2 coupled simulations of the Mid-Holocene and Last Glacial Maximum–Part 2: feedbacks with emphasis on the location of the ITCZ and mid-and high latitudes heat budget. Climate of the Past, 3(2), 279-296.

[4] Burbridge, R. E., Mayle, F. E., & Killeen, T. J. (2004). Fifty-thousand-year vegetation and climate history of Noel Kempff Mercado national park, Bolivian Amazon. Quaternary Research, 61(2), 215-230.

[5] Bush, M. B., & Silman, M. R. (2004). Observations on Late Pleistocene cooling and precipitation in the lowland Neotropics. Journal of Quaternary Science, 19(7), 677-684.

[6] Bush, M.B. (2017). Climate science: The resilience of Amazonian forests. Nature, 541(7636), 167.

512 [7] Martin Calvo, M., & Prentice, I. C. (2015). Effects of fire and CO2 on
513 biogeography and primary production in glacial and modern climates. New
514 Phytologist, 208(3), 987-994.

515 [8] Cardoso Da Silva, J. M., & Bates, J. M. (2002). Biogeographic Patterns
516 and Conservation in the South American Cerrado : A Tropical Savanna
517 Hotspot: The Cerrado, which includes both forest and savanna habitats, is
518 the second largest South American biome, and among the most threatened
519 on the continent. AIBS Bulletin, 52(3), 225-234.

520 [9] Carnaval, A. C., & Moritz, C. (2008). Historical climate modelling predicts
521 patterns of current biodiversity in the Brazilian Atlantic forest. Journal of
522 Biogeography, 35(7), 1187-1201.

523 [10] Claussen, M., Selent, K., Brovkin, V., Raddatz, T., & Gayler, V. (2013).
524 Impact of CO2 and climate on Last Glacial maximum vegetation–a factor
525 separation. Biogeosciences, 10, 3593-3604.

526 [11] Colinvaux, P. A., De Oliveira, P. E., Moreno, J. E., Miller, M. C., & Bush,
527 M. B. (1996). A long pollen record from lowland Amazonia: forest and
528 cooling in glacial times. Science, 274(5284), 85.

529 [12] Colinvaux, P. A., De Oliveira, P. E., & Bush, M. B. (2000). Amazonian
530 and neotropical plant communities on glacial time-scales: the failure of the
531 aridity and refuge hypotheses. Quaternary Science Reviews, 19(1), 141-169.

532 [13] Costa, L. P. (2003). The historical bridge between the Amazon and the
533 Atlantic Forest of Brazil: a study of molecular phylogeography with small
534 mammals. Journal of Biogeography, 30(1), 71-86.

535 [14] Cowling, S. A., Maslin, M. A., & Sykes, M. T. (2001). Paleovegetation
536 simulations of lowland Amazonia and implications for neotropical allopatry
537 and speciation. Quaternary Research, 55(2), 140-149.

[15] Cramer, W., Bondeau, A., Woodward, F. I., Prentice, I. C., Betts, R. A., Brovkin, V., ... & Kucharik, C. (2001). Global response of terrestrial ecosystem structure and function to CO2 and climate change: results from six dynamic global vegetation models. Global change biology, 7(4), 357-373.

[16] da Silva, J. M. C. (1995). Biogeographic analysis of the South American Cerrado avifauna. Steenstrupia, 21, 49-67.

[17] D'Apolito, C., Absy, M. L., & Latrubesse, E. M. (2013). The Hill of Six Lakes revisited: new data and re-evaluation of a key Pleistocene Amazon site. Quaternary Science Reviews, 76, 140-155.

[18] Fontes, D., Cordeiro, R. C., Martins, G. S., Behling, H., Turcq, B., Sifeddine, A., ... & Rodrigues, R. A. (2017). Paleoenvironmental dynamics in South Amazonia, Brazil, during the last 35,000 years inferred from pollen and geochemical records of Lago do Saci. Quaternary Science Reviews, 173, 161-180.

[19] Garzón-Orduña, I. J., Benetti-Longhini, J. E., & Brower, A. V. (2014). Timing the diversification of the Amazonian biota: butterfly divergences are consistent with Pleistocene refugia. Journal of biogeography, 41(9), 1631-1638.

[20] Haffer, J. (1969). Speciation in Amazonian forest birds. Science, 165(3889), 131-137.

[21] Haffer, J. R. (1997). Alternative models of vertebrate speciation in Amazonia: an overview. Biodiversity & Conservation, 6, 451-476.

[22] Hermanowski, B., da Costa, M. L., & Behling, H. (2012). Environmental changes in southeastern Amazonia during the last 25,000 yr revealed from a paleoecological record. Quaternary Research, 77(1), 138-148.

563 [23] Hopcroft, P. O., & Valdes, P. J. (2015). Last glacial maximum constraints
564   on the Earth System model HadGEM2-ES. Climate Dynamics, 45(5-6),
565   1657-1672.

566 [24] Kelley, D. I., Prentice, I. C., Harrison, S. P., Wang, H., Simard, M., Fisher,
567   J. B., & Willis, K. O. (2013). A comprehensive benchmarking system for
568   evaluating global vegetation models. Biogeosciences, 10, 3313-3340.

569 [25] Kelley, D. I., Harrison, S. P., & Prentice, I. C. (2014). Improved simulation
570   of fire–vegetation interactions in the Land surface Processes and eXchanges
571   dynamic global vegetation model (LPX-Mv1). Geoscientific Model Develop-
572   ment, 7(5), 2411-2433.

573 [26] Kelley, D. I., & Harrison, S. P. (2014). Enhanced Australian carbon sink
574   despite increased wildfire during the 21st century. Environmental Research
575   Letters, 9(10), 104015.

576 [27] Leite, R. N., & Rogers, D. S. (2013). Revisiting Amazonian phylogeography:
577   insights into diversification hypotheses and novel perspectives. Organisms
578   Diversity & Evolution, 13(4), 639-664.

579 [28] Marchant, R., Cleef, A., Harrison, S. P., Hooghiemstra, H., Markgraf, V.,
580   Van Boxel, J., ... & Behling, H. (2009). Pollen-based biome reconstructions
581   for Latin America at 0, 6000 and 18 000 radiocarbon years ago. Climate of
582   the Past, 5, 725-767.

583 [29] Martin Calvo, M., & Prentice, I. C. (2015). Effects of fire and CO2 on
584   biogeography and primary production in glacial and modern climates. New
585   Phytologist, 208(3), 987-994.

586 [30] Mayle, F. E., Beerling, D. J., Gosling, W. D., & Bush, M. B. (2004).
587   Responses of Amazonian ecosystems to climatic and atmospheric carbon
588   dioxide changes since the last glacial maximum. Philosophical Transactions
589   of the Royal Society of London. Series B: Biological Sciences, 359(1443),
590   499-514.

22

591 [31] Mayle, F. E., Burn, M. J., Power, M., & Urrego, D. H. (2009). Vegetation
592 and fire at the Last Glacial Maximum in tropical South America. In Past
593 climate variability in South America and surrounding regions (pp. 89-112).
594 Springer, Dordrecht.

595 [32] McMahon, S. M., Harrison, S. P., Armbruster, W. S., Bartlein, P. J., Beale,
596 C. M., Edwards, M. E., ... & Prentice, I. C. (2011). Improving assessment
597 and modelling of climate change impacts on global terrestrial biodiversity.
598 Trends in Ecology & Evolution, 26(5), 249-259.

599 [33] Moncrieff, G. R., Scheiter, S., Bond, W. J., & Higgins, S. I. (2014). In-
600 creasing atmospheric CO_2 overrides the historical legacy of multiple stable
601 biome states in Africa. New Phytologist, 201(3), 908-915.

602 [34] Monteith, J. L. (1995). A reinterpretation of stomatal responses to humid-
603 ity. Plant, Cell & Environment, 18(4), 357-364.

604 [35] Moritz, C., Patton, J. L., Schneider, C. J., & Smith, T. B. (2000). Di-
605 versification of rainforest faunas: an integrated molecular approach. Annual
606 review of ecology and systematics, 31(1), 533-563.

607 [36] O'ishi, R., & Abe-Ouchi, A. (2013). Influence of dynamic vegetation on
608 climate change and terrestrial carbon storage in the Last Glacial Maximum.

609 [37] Pennington, R. T., & Dick, C. W. (2010). Diversification of the Amazonian
610 flora and its relation to key geological and environmental events: a molecular
611 perspective. Blackwell.

612 [38] Prado, D. E., & Gibbs, P. E. (1993). Patterns of species distributions in
613 the dry seasonal forests of South America. Annals of the Missouri Botanical
614 Garden, 902-927.

615 [39] Prentice, I. C., Harrison, S. P., & Bartlein, P. J. (2011). Global vegetation
616 and terrestrial carbon cycle changes after the last ice age. New Phytologist,
617 189(4), 988-998.

[40] Prentice, I. C., Kelley, D. I., Foster, P. N., Friedlingstein, P., Harrison, S. P., & Bartlein, P. J. (2011). Modeling fire and the terrestrial carbon balance. Global Biogeochemical Cycles, 25(3).

[41] Adrian Quijada-Mascareñas, J., Ferguson, J. E., Pook, C. E., Salomao, M. D. G., Thorpe, R. S., & Wüster, W. (2007). Phylogeographic patterns of trans-Amazonian vicariants and Amazonian biogeography: the Neotropical rattlesnake (Crotalus durissus complex) as an example. Journal of Biogeography, 34(8), 1296-1312.

[42] Rothermel, R. C. (1972). A mathematical model for predicting fire spread in wildland fuels.

[43] Sitch, S., Smith, B., Prentice, I. C., Arneth, A., Bondeau, A., Cramer, W., ... & Thonicke, K. (2003). Evaluation of ecosystem dynamics, plant geography and terrestrial carbon cycling in the LPJ dynamic global vegetation model. Global Change Biology, 9(2), 161-185.

[44] Sitch, S., Huntingford, C., Gedney, N., Levy, P. E., Lomas, M., Piao, S. L., ... & Jones, C. D. (2008). Evaluation of the terrestrial carbon cycle, future plant geography and climate-carbon cycle feedbacks using five Dynamic Global Vegetation Models (DGVMs). Global Change Biology, 14(9), 2015-2039.

[45] Smith, B. T., Amei, A., & Klicka, J. (2012). Evaluating the role of contracting and expanding rainforest in initiating cycles of speciation across the Isthmus of Panama. Proceedings of the Royal Society B: Biological Sciences, 279(1742), 3520-3526.

[46] Stein, U., & Alpert, P. I. N. H. A. S. (1993). Factor separation in numerical simulations. Journal of the Atmospheric Sciences, 50(14), 2107-2115.

[47] Thonicke, K., Spessa, A., Prentice, I. C., Harrison, S. P., Dong, L., & Carmona-Moreno, C. (2010). The influence of vegetation, fire spread and

fire behaviour on biomass burning and trace gas emissions: results from a process-based model. Biogeosciences, 7(6), 1991.

[48] Werneck, F. P., Nogueira, C., Colli, G. R., Sites, J. W., & Costa, G. C. (2012). Climatic stability in the Brazilian Cerrado: implications for bio-geographical connections of South American savannas, species richness and conservation in a biodiversity hotspot. Journal of Biogeography, 39(9), 1695-1706.

[49] Wilson, J. B., & Agnew, A. D. (1992). Positive-feedback switches in plant communities. In Advances in ecological research (Vol. 23, pp. 263-336). Academic Press.

[50] Wuster, W., Ferguson, J. E., Quijada-Mascareñas, J. A., Pook, C. E., Da Graca Salomao, M., & Thorpe, R. S. (2005). Tracing an invasion: land-bridges, refugia, and the phylogeography of the Neotropical rattlesnake (Serpentes: Viperidae: Crotalus durissus). Molecular Ecology, 14(4), 1095-1108.

Corresponding Author

Dr. Hiromitsu Sato (hiromitsu.sato@mail.utoronto.ca)

Acknowledgments

Author Contributions

HS: Project lead, project design, performed experiment, analysis, and writing.

DIK: Project design, analysis, post-processing of data, figures, and writing.

SJM: Project design, analysis, and writing.

MMC: Development of model and execution of experiment.

SAC: Project design, analysis, and editing.

ICP: Model development, analysis, and writing.

Data Availability

The data and code that support the findings of this study are available here.

Code Availability

LPX is available at the following repository: https://bitbucket.org/teambcd/lpx
.

Competing Interest Statement

The authors declare no competing interests.

Figure Legend
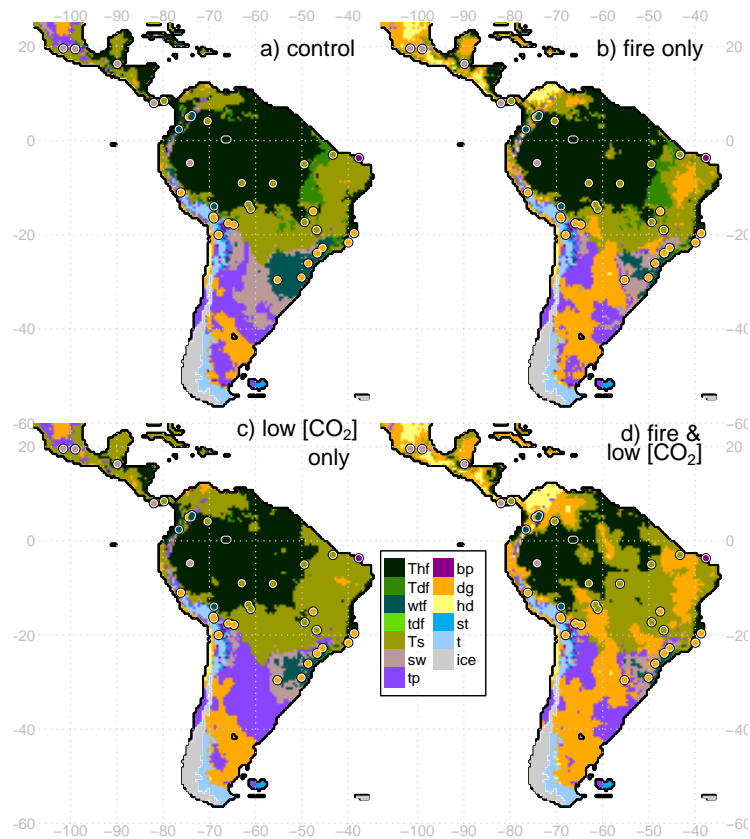
Figure 1: LPX model reconstructions of LGM biome distributions for four scenarios based on the average output from four driving AOGCM LGM climate reconstructions (ensemble experiment). 'Fire' indicates the presence of a process-based wildfire representation (b,d). 'Low CO_2' indicates scenarios with an LGM CO_2 of 180 ppm (c,d) rather than a Pre-Industrial CO_2 of 280 ppm. Dots represent the locations of pollen cores used to validate model reconstructions while colors indicate the biome reconstructed from the pollen spectra.

Thf = tropical humid forest, Tdf = tropical dry forest, Ts = tropical savanna, sw = sclerophyll woodland, tp = temperate parkland, bp = boreal parkland, dg = dry grass/shrubland, hd = hot desert, st = shrub tundra, t = tundra
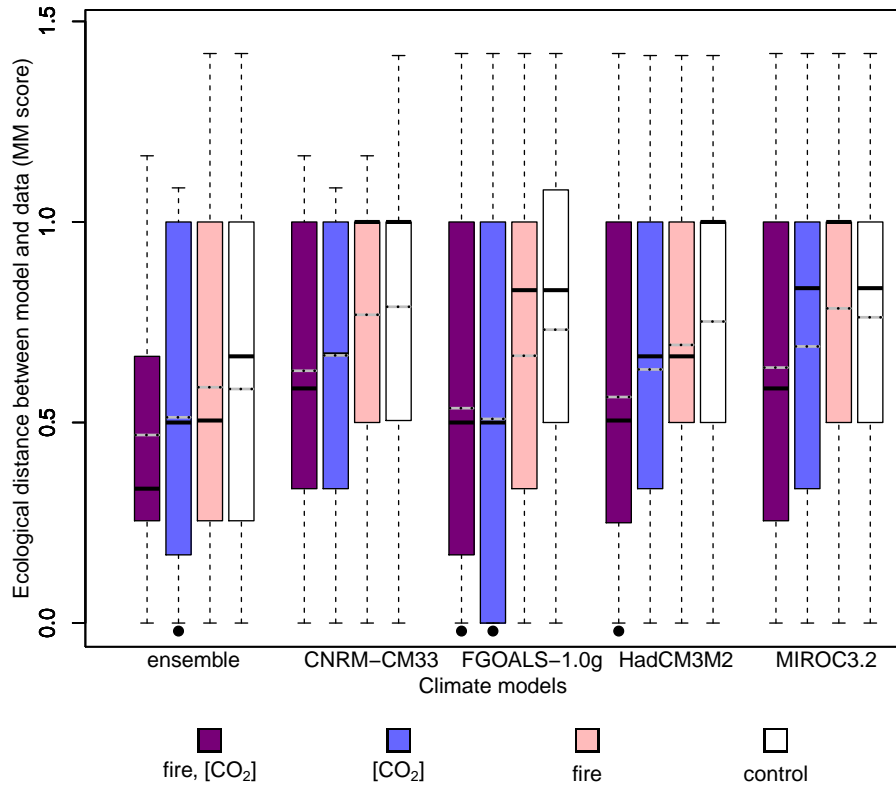
Figure 2: Statistical comparison between model reconstructions and pollen cores. Summary of model-data comparison of scenarios from the fire/low CO_2 factorial experiment for each LGM climate reconstruction, performed by comparing biome reconstructions by LPX with site-based pollen reconstructions of biomes by the Discrete Manhattan Metric (DMM). The DMM a measure of the ecological distance between biome types (methods). Scenarios with solid black bars at bottom are not significantly different from *fire and low CO_2* ensemble scenario, based on a $p > 0.1$ cutoff using a paired T-test over all sites. Dashed bars are the mean of DMM point scores (scenario score) and solid bars are the median of DMM point scores. Boxes denote interquartile range while whiskers denote minimum and maximum DMM point scores with an experiment scenario.
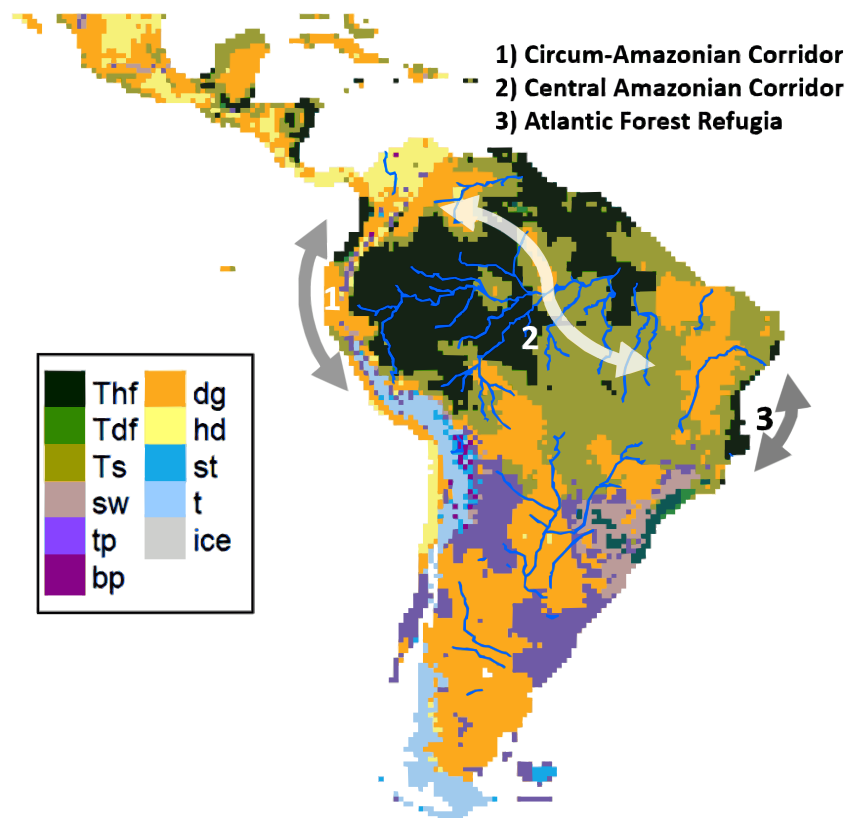
Figure 3: Identification of reconstructed biogeographical formations in the ensemble *fire and low CO₂* scenario. Corridors are hypothesized past open vegetation formations that are theorized to have facilitated dispersal during glacial periods, while refugia are stable forested regions that remained robust against past climatic change.
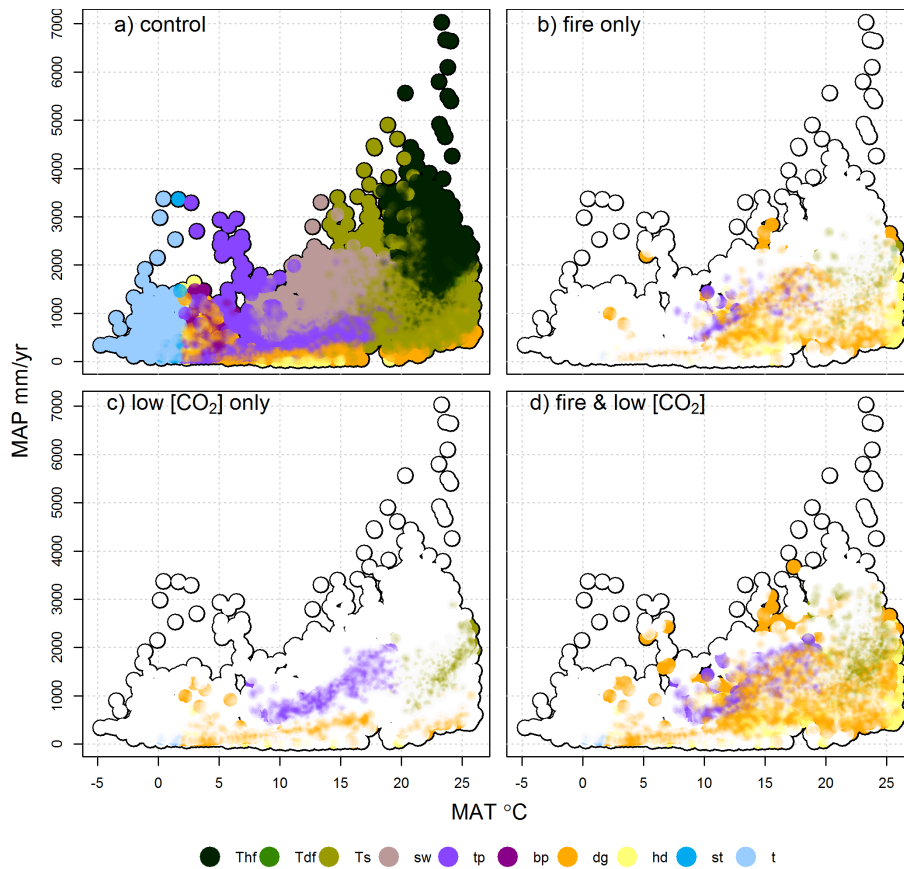
Figure 4: The effects of fire and low CO_2 on climate-vegetation relationships. Whittaker plots showing biomes in the climate space of mean annual temperature (MAT) and mean annual precipitation (MAP) for four scenarios in the fire/CO_2 factorial experiment. All of biome space is shown for the control scenario (a), while for *fire only* (b), *low CO_2 only* (c), and *fire and low CO_2* (d), points that are identical to control scenario are left white while coloured points represent shifts due to fire and low CO_2.
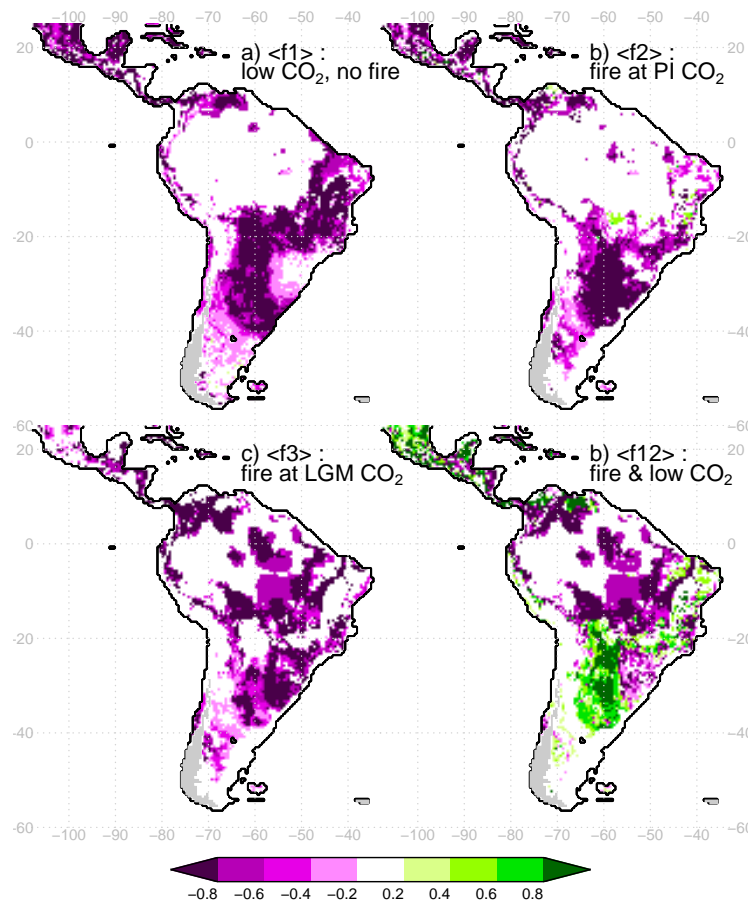
Figure 5: The individual and interactive effects of fire and CO_2 on tree cover. Results from the Stein-Alpert Decomposition showing the responses of tree cover to the a) direct impact of CO_2, b) direct impact of fire c) combined impacts of fire and CO_2, and d) purely interactive impacts of CO_2. Purple regions show losses in tree cover due to a specific factor while green shows increases.
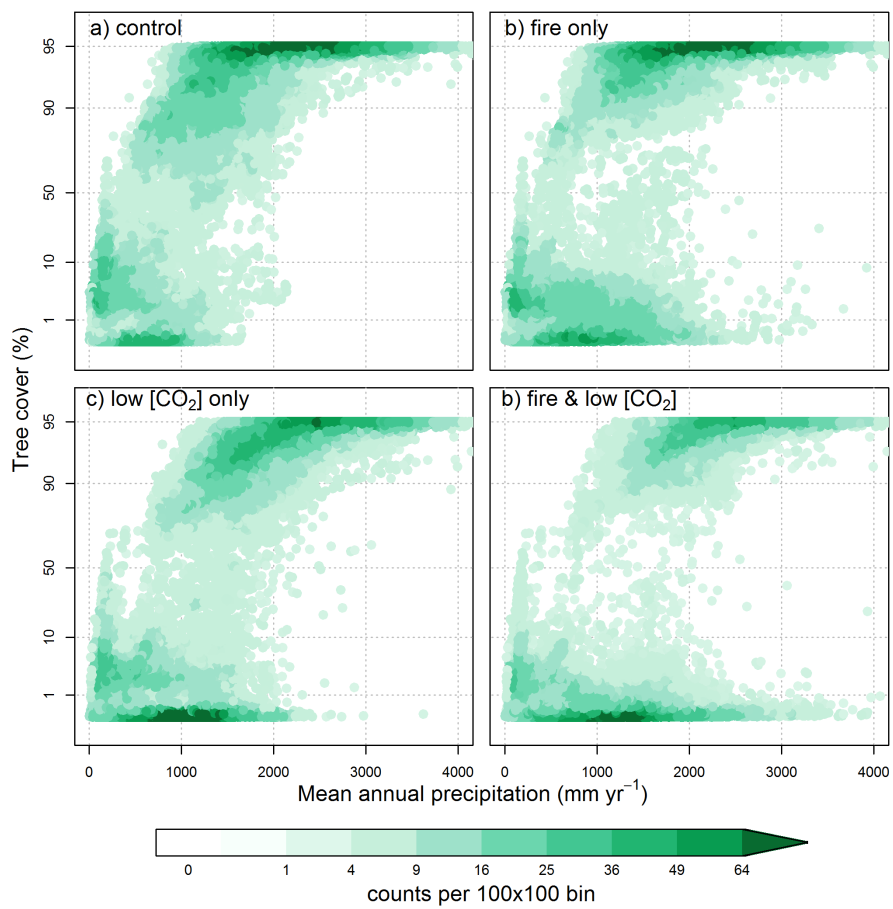
Figure 6: The effects of fire and low CO_2 on the bimodality of tree cover. Fractional tree cover against mean annual precipitation aggregated by runs driven by all four AOGCM LGM reconstructions to understand how fire and CO_2 mediate the moisture-tree cover relationship.

Methods-Only References

References

[1] Argollo, J., & Mourguiart, P. (2000). Late Quaternary climate history of the Bolivian Altiplano. Quaternary International, 72(1), 37-51.

[2] Barberi, M., Salgado-Labouriau, M. L., & Suguio, K. (2000). Paleovegetation and paleoclimate of "Vereda de Águas Emendadas", central Brazil. Journal of South American Earth Sciences, 13(3), 241-254.

[3] Behling, H. (1997). Late Quaternary vegetation, climate and fire history from the tropical mountain region of Morro de Itapeva, SE Brazil. Palaeogeography, Palaeoclimatology, Palaeoecology, 129(3-4), 407-422.

[4] Behling, H., & Lichte, M. (1997). Evidence of dry and cold climatic conditions at glacial times in tropical southeastern Brazil. Quaternary research, 48(3), 348-358.

[5] Behling, H., & Hooghiemstra, H. (1999). Environmental history of the Colombian savannas of the Llanos Orientales since the Last Glacial Maximum from lake records El Pinal and Carimagua. Journal of Paleolimnology, 21(4), 461-476.

[6] Behling, H., & Negrelle, R. R. (2001). Tropical rain forest and climate dynamics of the Atlantic lowland, Southern Brazil, during the Late Quaternary. Quaternary Research, 56(3), 383-389.

[7] Behling, H. (2002). South and southeast Brazilian grasslands during Late Quaternary times: a synthesis. Palaeogeography, Palaeoclimatology, Palaeoecology, 177(1-2), 19-27.

[8] Behling, H., Arz, H. W., Pätzold, J., & Wefer, G. (2002). Late Quaternary vegetational and climate dynamics in southeastern Brazil, inferences from

marine cores GeoB 3229-2 and GeoB 3202-1. Palaeogeography, Palaeoclimatology, Palaeoecology, 179(3-4), 227-243.

[9] Behling, H., Pillar, V. D., Orlóci, L., & Bauermann, S. G. (2004). Late Quaternary Araucaria forest, grassland (Campos), fire and climate dynamics, studied by high-resolution pollen, charcoal and multivariate analysis of the Cambará do Sul core in southern Brazil. Palaeogeography, Palaeoclimatology, Palaeoecology, 203(3-4), 277-297.

[10] Behling, H., Pillar, V. D., & Bauermann, S. G. (2005). Late Quaternary grassland (Campos), gallery forest, fire and climate dynamics, studied by pollen, charcoal and multivariate analysis of the São Francisco de Assis core in western Rio Grande do Sul (southern Brazil). Review of palaeobotany and palynology, 133(3-4), 235-248.

[11] Chepstow-Lusty, A., Bush, M. B., Frogley, M. R., Baker, P. A., Fritz, S. C., & Aronson, J. (2005). Vegetation and climate change on the Bolivian Altiplano between 108,000 and 18,000 yr ago. Quaternary Research, 63(1), 90-98.

[12] del Socorro Lozano-Garcia, M., & Ortega-Guerrero, B. (1994). Palynological and magnetic susceptibility records of Lake Chalco, central Mexico. Palaeogeography, Palaeoclimatology, Palaeoecology, 109(2-4), 177-191.

[13] del Socorro Lozano-García, M., & Ortega-Guerrero, B. (1998). Late Quaternary environmental changes of the central part of the Basin of Mexico; correlation between Texcoco and Chalco basins. Review of Palaeobotany and Palynology, 99(2), 77-93.

[14] Graf, K. (1992). Pollendiagramme aus den Anden: Eine Synthese zur Klimageschichte und Vegetationsentwicklung seit der letzten Eiszeit. Universität Zürich-Irchel-Geographisches Institut.

[15] Guimarães, J. T. F., Rodrigues, T. M., Reis, L. S., de Figueiredo, M. M. J. C., da Silva, D. F., Alves, R., ... & Sahoo, P. K. (2017). Modern pollen rain

747 as a background for palaeoenvironmental studies in the Serra dos Carajás,

748 southeastern Amazonia. The Holocene, 27(8), 1055-1066.

749 [16] Hansen, B. C. S., Rodbell, D. T., Seltzer, G. O., Leon, B., Young, K. R., &

750 Abbott, M. (2003). Late-glacial and Holocene vegetational history from two

751 sites in the western Cordillera of southwestern Ecuador. Palaeogeography,

752 Palaeoclimatology, Palaeoecology, 194(1-3), 79-108.

753 [17] Hooghiemstra, H., Cleef, A. M., Noldus, C. W., & Kappelle, M. (1992). Up-

754 per Quaternary vegetation dynamics and palaeoclimatology of the La Chonta

755 bog area (Cordillera de Talamanca, Costa Rica). Journal of Quaternary Sci-

756 ence, 7(3), 205-225.

757 [18] Ledru, M. P., Braga, P. I. S., Soubiès, F., Fournier, M., Martin, L., Suguio,

758 K., & Turcq, B. (1996). The last 50,000 years in the Neotropics (Southern

759 Brazil): evolution of vegetation and climate. Palaeogeography, Palaeoclima-

760 tology, Palaeoecology, 123(1-4), 239-257.

761 [19] Ledru, M. P., Cordeiro, R. C., Dominguez, J. M. L., Martin, L., Mour-

762 guiart, P., Sifeddine, A., & Turcq, B. (2001). Late-Glacial cooling in Ama-

763 zonia inferred from pollen at Lagoa do Caçó, Northern Brazil. Quaternary

764 Research, 55(1), 47-56.

765 [20] Ledru, M. P., Mourguiart, P., & Riccomini, C. (2009). Related changes

766 in biodiversity, insolation and climate in the Atlantic rainforest since the

767 last interglacial. Palaeogeography, Palaeoclimatology, Palaeoecology, 271(1-

768 2), 140-152.

769 [21] Leyden, B. W. (1984). Guatemalan forest synthesis after Pleistocene arid-

770 ity. Proceedings of the National Academy of Sciences, 81(15), 4856-4859.

771 [22] Mayle, F. E., Burbridge, R., & Killeen, T. J. (2000). Millennial-scale dy-

772 namics of southern Amazonian rain forests. Science, 290(5500), 2291-2294.

[23] Mayle, F. E., Burn, M. J., Power, M., & Urrego, D. H. (2009). Vegetation and fire at the Last Glacial Maximum in tropical South America. In Past climate variability in South America and surrounding regions (pp. 89-112). Springer, Dordrecht.

[24] Mourguiart, P., Argollo, J., & Wirrmann, D. (1995). Evolución del lago Titicaca desde 25000 anos BP.

[25] Mourguiart, P., & Ledru, M. P. (2003). Last glacial maximum in an Andean cloud forest environment (Eastern Cordillera, Bolivia). Geology, 31(3), 195-198.

[26] Oliveira, P. E. D. (1992). A palynological record of late Quaternary vegetational and climatic change in southeastern Brazil (Doctoral dissertation, The Ohio State University).

[27] Pessenda, L. C. R., De Oliveira, P. E., Mofatto, M., de Medeiros, V. B., Garcia, R. J. F., Aravena, R., ... & Etchebehere, M. L. (2009). The evolution of a tropical rainforest/grassland mosaic in southeastern Brazil since 28,000 14 C yr BP based on carbon isotopes and pollen records. Quaternary Research, 71(3), 437-452.

[28] Piperno, D. R., Bush, M. B., & Colinvaux, P. A. (1991). Paleoecological perspectives on human adaptation in central Panama. I. The Pleistocene. Geoarchaeology, 6(3), 201-226.

[29] Salgado-Labouriau, M. L., Barberi, M., Ferraz-Vicentini, K. R., & Parizzi, M. G. (1998). A dry climatic event during the late Quaternary of tropical Brazil. Review of Palaeobotany and Palynology, 99(2), 115-129.

[30] Urrego, D. H., Bush, M. B., & Silman, M. R. (2010). A long history of cloud and forest migration from Lake Consuelo, Peru. Quaternary Research, 73(2), 364-373.

[31] Van der Hammen, T., & González, E. (1960). Upper pleistocene and holocene climate and vegetation of the "Sabana de Bogota"(Colombia, South America). Leidse Geologische Mededelingen, 25(1), 261-315.

[32] Van der Hammen, T., & Absy, M. L. (1994). Amazonia during the last glacial. Palaeogeography, palaeoclimatology, palaeoecology, 109(2-4), 247-261.

[33] van der Hammen, T., & Hooghiemstra, H. (2003). Interglacial–glacial Fuquene-3 pollen record from Colombia: an Eemian to Holocene climate record. Global and Planetary Change, 36(3), 181-199.

[34] Van Geel, B., & Van der Hammen, T. (1973). Upper Quaternary vegetational and climatic sequence of the Fuquene area (Eastern Cordillera, Colombia). Palaeogeography, Palaeoclimatology, Palaeoecology, 14(1), 9-92.

[35] Watts, W. A., & Bradbury, J. P. (1982). Paleoecological Studies at Lake Patzcuaro on the West-Central Mexican Plateau and at Chalco in the Basin of Mexico 1. Quaternary Research, 17(1), 56-70.

[36] Wille, M., Negret, J. A., & Hooghiemstra, H. (2000). Paleoenvironmental history of the Popayán area since 27 000 yr BP at Timbio, southern Colombia. Review of Palaeobotany and Palynology, 109(1), 45-63.

Extended Data
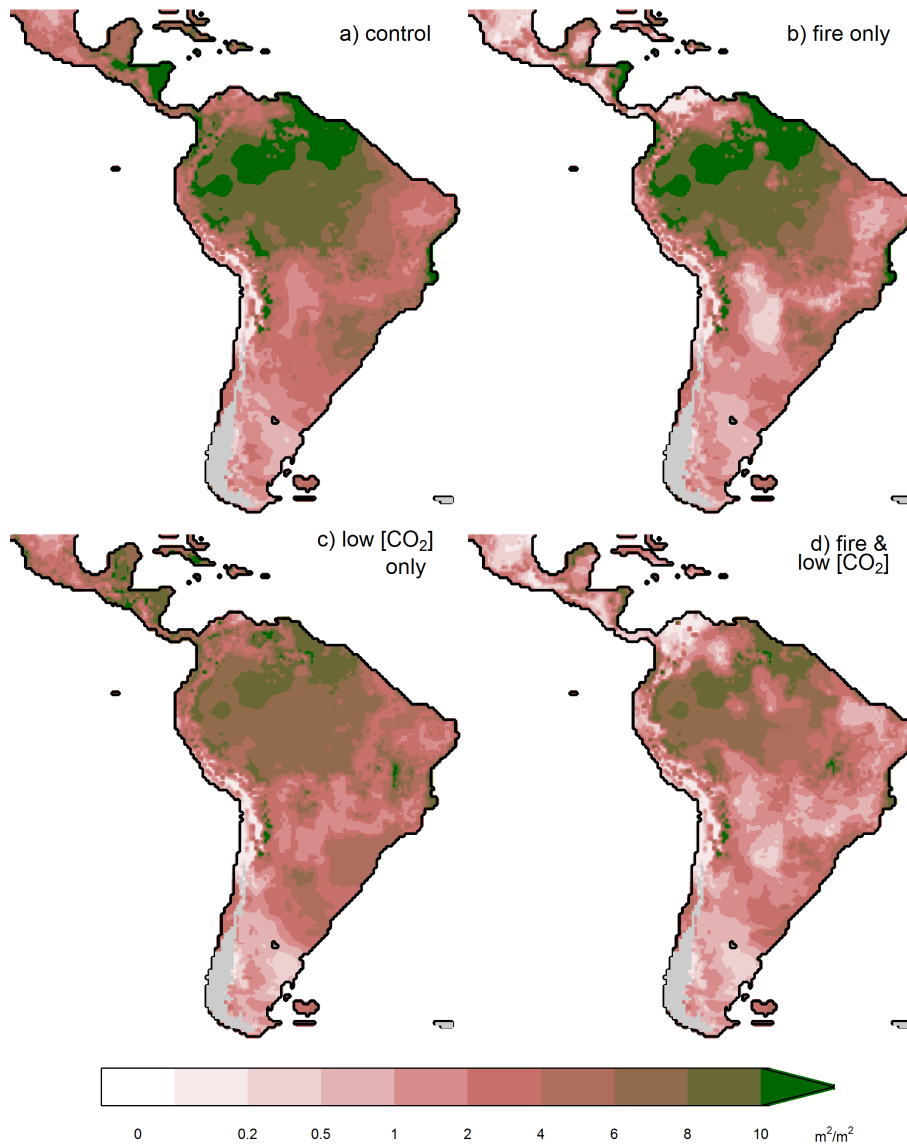
Figure 1: Canopy density (leaf area index) distributions for the ensemble factorial experiment in dimensionless units (m^2/m^2).
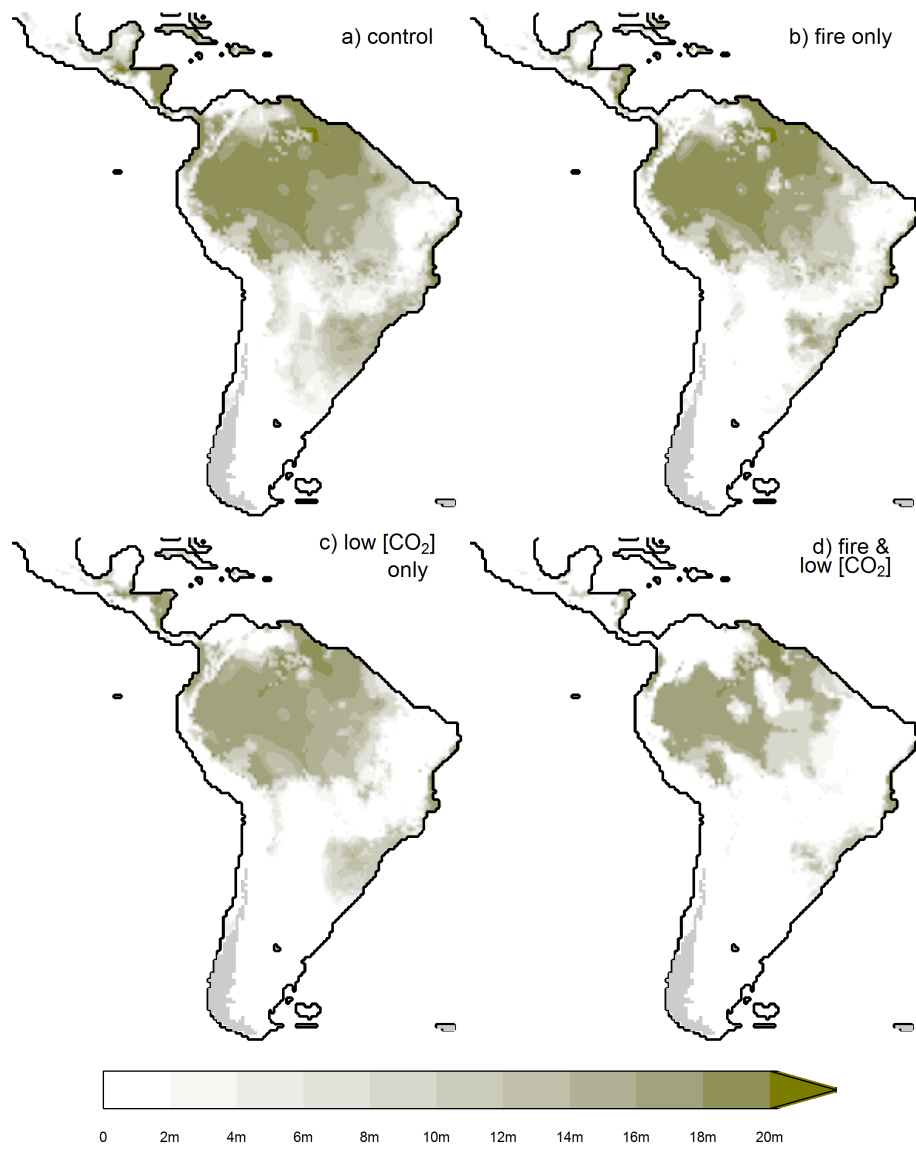
Figure 2: Canopy height (metres) distributions for the ensemble factorial experiment.
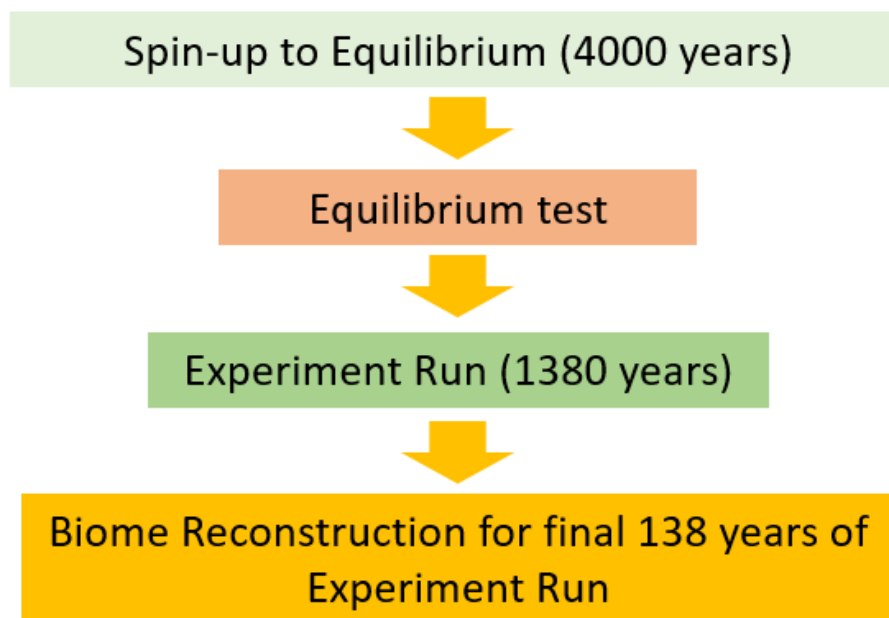
Figure 3: Flow of model protocol from spin-up to biome assignment for each factorial experiment run (LGM climate reconstruction + factorial experiment conditions)

a) GDD > 350

		Forest
Desert	Dry Grassland-Shrubland	10m
		Savanna

Height — FPC — 0, 0.3, 0.6

GDD < 350

	Forest
Tundra	10m
	Shrub Tundra

Height — FPC — 0, 0.6

b)

Tropical	Tropical PFT present in cell	Tropical Forest	Tropical Savanna
Warm Temperate	Temperate Broadleaf Evergreen pft fpc greater than 50 % of total fpc	Warm Temperate Forest	Sclerophyll Woodland
Temperate	Temperate Needle Evergreen or Temperate Broadleaf Summergreen pft present	Temperate Forest	Temperate Parkland
Boreal	Not Tropical, Warm Temperate, or Temperate	Boreal Forest	Boreal Parkland

c)

Larger proportion of evergreen pfts than combined summergreen and raingreen pfts	Tropical Humid Forest	Temperate Evergreen Forest	Boreal Evergreen Forest
Larger proportion of combined summergreen and raingreen pfts than evergreen pfts	Tropical Dry Forest	Temperate Deciduous Forest	Boreal Evergreen Forest

Figure 4: Diagram representing the biome assignment scheme. a) Division of cold and warm-hot biomes according to GDD and general organization of biomes according by fpc and height. b) Classification into more specific biomes by presence and dominance of pfts. c) Further classification of forests into seasonal and evergreen categories based on pft proportions.

Site Name	Latititude	Longitude	Country	Pollen Biome	Reference
Lake Patsucuarco	19.6	-101.58	Mexico	9	[35]
Chalco Lake	19.5	-99	Mexico	9	[12]
Lake Texcoco	19.4	-99	Mexico	9	[13]
Lake Quexil	16.3	-89.9	Guatemala	9	[21]
El Valle	8.43	-79.8	Panama	8	[28]
La Chonta	8	-82	Costa Rica	9	[17]
Fuquene II	5.45	-73.77	Colombia	3	[33]
Agua Blanca	5	-74.45	Colombia	12	[14]
Herrera	5	-73.9	Colombia	3	[34]
El Pinal	4.1	-70.4	Colombia	8	[5]
Timbio	2.4	-76.6	Colombia	3	[36]
Lagoa Das Patas	0.26	-66.7	Brazil	1	[26]
Lake Pata	0.26	-66.1	Brazil	1	[5]
Lagoa de Caco	-2.97	-43.3	Brazil	8	[19][17]
GeoB 3104-1	-3.67	-37.7	Ocean	11	[8]
Ciudad Universitaria	-4.75	-74.2	Colombia	3	[31]
Serra Sul Carajas	-5	-49.5	Brazil	8	[15]
Katira	-9	-63	Brazil	8	[32]
Lago do Saci	-9.1	-56.3	Brazil	8	[18]
Laguna Junin	-11	-76.2	Peru	12	[16]
Laguna Bella Vista	-13.6	-61.56	Bolivia	3	[22]
Consuelo	-13.95	-68.9	Peru	8	[30]
Chaplin	-14.5	-61.1	Bolivia	12	[4]
Aguas Emendadas	-15	-47.6	Brazil	12	[2]
Titicaca	-16.1	-69.2	Bolivia/Peru	12	[24]
Lake Huinamimarca	-16.5	-69	Bolivia	12	[25]
Crominia	-17.3	-49.4	Brazil	8	[29]
Wasa Mayu	-17.54	-65.9	Bolivia	12	[14]
Siberia	-17.8	-64.7	Bolivia	12	[25]
Salitre	-19	-46.8	Brazil	12	[18]
Serra Negra	-18.95	-46.85	Brazil	8	[26]
GeoB 3229-2	-19.63	-38.7	Brazil	12	[8]
Salar de Uyuni	-20	-68	Bolivia	12	[11]
Catas Altas	-20.1	-43.4	Brazil	12	[4]
GeoB 3202-1	-21.6	-39.9	Brazil	12	[7]
Morro de Itapeva	-22.8	-45.5	Brazil	12	[3]
Colonia	-23.9	-46.7	Brazil	12	[20]
Curucutu	-23.9	-46.7	Brazil	12	[27]
Volta Velha	-26.1	-48.6	Brazil	12	[6]
Cambara Sol	-29.1	-50.1	Brazil	12	[9]
Sao Francisco	-29.6	-55.3	Brazil	12	[10]

Table 1: List of original palynological studies used in conjunction with meta-analyses by Marchant et al. [28] and Mayle et al.[23] for 18 000 ± 1000 ^{14}C yr BP. 1:tropical humid forest, 2:tropical dry forest, 3: warm temperate forest, 4: temperate evergreen forest, 5: temperate deciduous forest, 6: boreal evergreen forest, 7: boreal deciduous forest, 8: tropical savanna, 9: sclerophyll woodland, 10: temperate parkland, 11: boreal parkland, 12: dry grass/shrubland 13: hot desert, 14: shrub tundra, 15: tundra

Biome	Dense	Sparse	Tall	Short	Hot	Cold	Seasonal	Evergreen
Thf	1	0	1	0	1	0	0	1
Tdf	1	0	1	0	1	0	1	0
wtf	1	0	1	0	2/3	1/3	1/2	1/2
tef	1	0	1	0	1/3	2/3	0	1
tdf	1	0	1	0	1/3	2/3	1	0
bef	1	0	1	0	0	1	0	1
bdf	1	0	1	0	0	1	1	0
Ts	2/3	1/3	0	1	1	0	2/3	1/3
sw	2/3	1/3	0	1	2/3	1/3	1/2	1/2
tp	2/3	1/3	0	1	1/3	2/3	1/2	1/2
bp	2/3	1/3	0	1	0	1	1/2	1/2
g	1/3	2/3	0	1	1	0	1/2	1/2
d	0	1	0	1	1	0	1/2	1/2
st	1/3	2/3	0	1	0	1	1/2	1/2
t	0	1	0	1	0	1	1/2	1/2

Table 2: Affinity matrix for LPX biomes to compute 'distance' between biomes in trait space. Thf = Tropical humid forest, Tdf = Tropical dry forest, wtf = warm temperate forest, tef = temperate evergreen forest, tdf = temperate deciduous forest, bef = boreal evergreen forest, bdf = boreal deciduous forest, Ts = Tropical savanna, sw = sclerophyll woodland, tp = temperate parkland, bp = boreal parkland, g = dry grass/shrubland, d = desert, st = shrub tundra, t = tundra

Pollen Reconstructed Biomes	**Model Assigned Biomes**
Tropical Rainforest	Tropical Humid Forest
Tropical Seasonal Forest	Tropical Dry Forest
Cerrado	Tropical Savanna
Caatinga	Dry Grass-Shrublands
Steppe	
Desert	Hot Desert

Table 3: Correspondence legend between pollen reconstructed and model assigned biomes.